

with $W(T_R) = \epsilon T_R - T_R \mu (\partial \ln Z_1 / \partial \mu)_{T, \Lambda}$ and $\zeta(T_R) = \mu (\partial \ln Z / \partial \mu)_{T, \Lambda}$. From Eq. (12) one sees that $W = \epsilon T_R - (2\pi)^{-1} T_R^2 + O(T_R^3, \epsilon T_R^2)$, and $\zeta = (2\pi)^{-1} T_R + O(T_R^2, \epsilon T_R)$. As usual, T_c is given by the zero of W ; as expected $T_c = 2\pi\epsilon + O(\epsilon^2)$, which is the correct result for the classical three-component model.³ The exponent ν can be defined as in Ref. 3 and so has the same value (since W is the same). One other independent exponent must be checked. We will check η because note that η does not correspond to the power-law behavior of Γ_2 at T_c . Consider the magnetization, Eq. (8), in the unrenormalized theory. With a constant magnetic field h in the z direction, the bare propagator becomes $ST/(k^2 + |h|)$, and so Eq. (8) gives $m(T_c, h) = -1 - (4\pi)^{-1} T_c \ln|h|$; this is the ϵ expansion of $-|h|^{1/\delta}$ with $\delta = 2\epsilon^{-1}$, and so $\eta + \epsilon + O(\epsilon^2)$ from hyperscaling. This is also the correct result. In addition, we could define an expo-

nent $\bar{\eta} \neq \eta$ via $\Gamma_2^R(T_c) \sim \mu^\epsilon k^2 (k/\mu)^{-\bar{\eta}}$ and μ replaced by Λ in the unrenormalized theory. Then, Eq. (15) implies $\bar{\eta} = \epsilon - \zeta(T_c)$, so that $\bar{\eta} = 0 + O(\epsilon^2)$. This last result is due to the lack of a singular self-energy contribution until two-loop order exactly as in ϕ^4 theory near four dimensions.

This work was supported by a National Science Foundation grant at the University of California, Santa Cruz, California 95064.

¹*Phase Transitions and Critical Phenomena*, edited by C. Domb and M. S. Green (Academic, New York, 1974), Vol. III.

²F. J. Dyson, Phys. Rev. **102**, 1217, 1230 (1956).

³E. Brézin and J. Zinn-Justin, Phys. Rev. B **14**, 3110 (1976), and Phys. Rev. Lett. **36**, 691 (1976).

⁴E. Brézin, J. Zinn-Justin, and J. C. Le Guillou, Phys. Rev. D **14**, 2615 (1976).

Observation of the Nuclear Acoustic Resonance of Hydrogen in NbH_{0.026}

H. I. Ringermacher, R. E. Norberg, and R. K. Sundfors

Department of Physics, Washington University, St. Louis, Missouri 63130

and

D. G. Westlake

Argonne National Laboratory, Argonne, Illinois 60439

(Received 22 January 1979)

Nuclear acoustic resonance of interstitial solute hydrogen has been observed in a single crystal of the transition metal niobium at 300 K and 49 kG. The resonance line has a demagnetization-dominated width of 0.4 G and a negative Knight shift of (8 ± 4) ppm.

We report the first observation of nuclear acoustic resonance (NAR) for hydrogen in a metal, in this case Nb. The dominant resonant dynamic interaction between acoustic waves and the interstitial ¹H spin system as well as with the ⁹³Nb nuclear spin system of the host metal is the Alpher-Rubin (A-R) effect^{1,2} which generates a local rf magnetic field associated with the acoustic standing wave established in the specimen. The local rf field is the acoustic analog of the externally applied \vec{H}_1 field in NMR, but avoids the rf skin-effect limitations inherent in NMR experiments on bulk conducting samples. The experiment was performed at 300 K and $\omega/2\pi = 210$ MHz in a superconducting solenoid at 49 kG. A composite resonator was prepared consisting of (i) a 3N+pure (> 99.9% purity), cylindrical Nb single crystal, 1.28 cm diam and 0.83 cm long

with axis along [110] and end faces ground optically flat and parallel, (ii) a 0.635 cm diam, 43-MHz fundamental, overtone-polished, x -cut quartz transducer operated at the fundamental and fifth harmonic, and (iii) a Canada Balsam resin bond. The specimen was reacted with hydrogen gas during cooling from 800°C to obtain a single crystal of Nb-H solid solution with a H concentration of 2.6 at.%.

A reflection mode technique,³ employing a hybrid junction uhf bridge spectrometer,⁴ was used together with diode detection. Precautions were taken to eliminate extraneous proton sources from the probe since the system was capable of observing stray NMR pickup as well as NAR signals. To ensure long-term acoustic stability it was necessary to retain the Canada Balsam bond as the only remaining significant source of NMR

protons. Field modulation and lockin detection at 100 Hz together with digital averaging were used for signal enhancement. The spectrometer was frequency locked, using FM techniques, and the crystal was temperature controlled to within 10 mK/h.

A characteristic of NAR A-R line shapes is the appearance of an admixture of absorptive and dispersive parts of the nuclear susceptibility. The resonant A-R acoustic absorption is given by²

$$\Delta\alpha = \frac{\omega B_0^2 \sin^2\theta \cos^2\theta}{2\rho v_l^3} \times \left[\frac{1-\beta^2}{(1+\beta^2)^2} \right] \left[\chi'' - \left(\frac{2\beta}{1-\beta^2} \right) \chi' \right], \quad (1)$$

where ρ is the metal density, v_l is the longitudinal sound velocity, and θ is the angle between the direction of wave propagation and the field \vec{B}_0 . χ'' and χ' are the usual dynamic Bloch susceptibilities for the hydrogen spin system. β is the "phase-shift factor" given by $\beta = \omega c^2 / 4\pi\sigma v_l^2$, where σ_0 is the dc conductivity in inverse seconds. For the present experiment the admixture is predominantly absorptive ($\chi'' + 0.3\chi'$) and the anticipated change in absorption arising from the 2.6% protons is calculated to be $4 \times 10^{-9} \text{ cm}^{-1}$.

To ensure that the spectrometer had sufficient sensitivity to detect such a small signal, the ^{93}Nb NAR of the host metal was first examined. Figure 1 shows the ^{93}Nb A-R derivative signal at 43 MHz and 300 K for a single sweep through resonance. The predominantly dispersive admixture present at 43 MHz is given by $\chi'' + 4.2\chi'$ and is confirmed by the observed line shape of Fig. 1. The ^{93}Nb

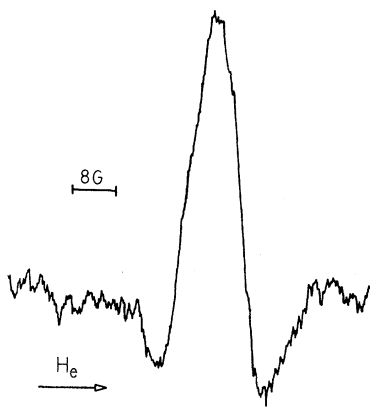


FIG. 1. The ^{93}Nb NAR A-R derivative signal as a function of applied external magnetic field \vec{H}_e . [Modulation field = 4 G (peak to peak) at 37 Hz, time constant = 10 sec.]

signal-to-noise ratio is comparable to that reported earlier for a marginal-oscillator experiment by Buttet⁵ and represents an attenuation change of $\Delta\alpha \approx 6 \times 10^{-7} \text{ cm}^{-1}$.

Figure 2 shows the observed 210-MHz ^1H NAR A-R derivative signal in $\text{NbH}_{0.026}$ for an accumulation of 192 sweeps at 72 sec/sweep. As expected, the line shape shows the aforementioned admixture of χ'' and χ' ; however, there are present additional features including a down-field "bump" and the 0.4-G (peak-to-peak) linewidth which can only be explained by including demagnetization effects arising from the surface geometry of the metal sample. A more detailed discussion of demagnetization effects on narrow lines in metals NAR is presented elsewhere.⁶ The proton line shape based on an inhomogeneously broadened Lorentzian admixture distorted by demagnetization effects, calculated for our crystal shape, is shown by the circles of Fig. 2. The demagnetization field variation over the acoustically excited region in the metal exceeded by more than an order of magnitude the superconducting solenoid field inhomogeneity of 0.1 G. Calculations show that the features on the downfield side of the line arise from protons far off the cylindrical sample axis. Their enhancement relative to the calculated shape may indicate that the acoustic power distribution was not quite uniform⁶ or was beyond the transducer boundary. The poorer fit on the upfield side was observed to be associated with a curving baseline from the broad Canada Balsam NMR pickup mentioned earlier.

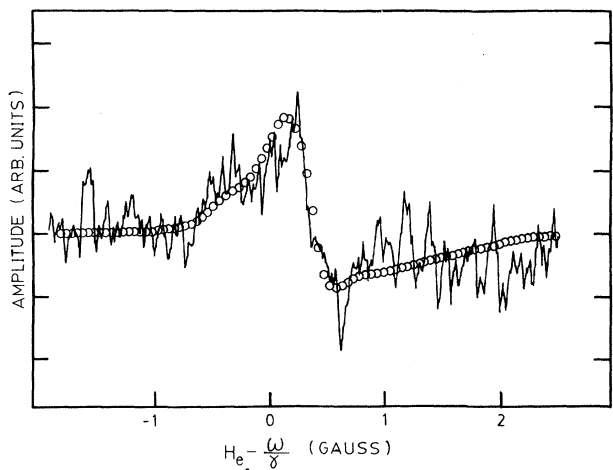


FIG. 2. The observed and calculated (circles) ^1H NAR A-R derivative lines as a function of applied external magnetic field \vec{H}_e . [Modulation field = 0.3 G (peak to peak) at 100 Hz, time constant = 0.3 sec.]

Besides affecting line shape, the demagnetizing field affects the shift which arises from bulk sample paramagnetism. Such shifts already have been considered in the NMR of hydrogen in metals⁷⁻⁹ and can be the source of considerable error in Knight-shift determinations. The shift is apparent in Fig. 2 from the location of the calculated signal crossover 0.4 G upfield from "zero" where it would have been were the protons "free." The total shift of the hydrogen line relative to a doped water reference was found to be $+0.8 \pm 0.2$ G. Correcting for the calculated demagnetization shift results in a net (negative) Knight shift of 0.4 ± 0.2 G upfield from the H₂O reference, or $|\Delta H/H| = (0.8 \pm 0.4) \times 10^{-3}\%$. Zamir and Cotts¹⁰ have reported, at 4 kG, zero shift of NbH_{0.05} and a negative shift of $1.6 \times 10^{-3}\%$ for all higher concentrations. The NAR ¹H line saturated rather easily, which is consistent with the anticipated¹¹ proton T_1 of about 0.2 sec.

The nonresonant A-R absorption modulation signal given by,

$$\Delta\alpha = \frac{\sigma_0 B_0 H_m \sin^2\theta}{\rho v_1 c^2} \left(\frac{\beta^2}{1 + \beta^2} \right), \quad (2)$$

where H_m is the modulation field, was used as an absolute attenuation calibration reference¹² and served also as a standard to establish optimum spectrometer tuning at all crystal angles. With the use of this method as a sensitivity check, the hydrogen NAR was examined at 0°, 45°, and 90°. The ¹H signal vanished at 0° and 90° as expected from Eq. (1) while the nonresonant A-R signal peaked at 90° as expected from Eq. (2). The maximum hydrogen NAR signal of Fig. 2 occurred at

45°. From the integrated line intensity and the A-R modulation calibration we find the absolute attenuation of the observed proton NAR signal to be $\Delta\alpha \approx 2 \times 10^{-8} \text{ cm}^{-1}$. This agrees reasonably well with the calculated value considering that the observed shape is not a Lorentzian.

We are grateful to D. I. Bolef, M. Conradi, and P. A. Fedders for stimulating discussions. This work was supported in part by the National Science Foundation and by the U. S. Department of Energy.

¹R. A. Alpher and R. J. Rubin, *J. Acoust. Soc. Am.* **26**, 452 (1954).

²P. A. Fedders, *Phys. Rev. B* **7**, 1739 (1973).

³D. I. Bolef and J. G. Miller, *Physical Acoustics* (Academic, New York, 1971), Vol. 8, Chap. 3.

⁴M. P. Klein and D. E. Phelps, *Rev. Sci. Instrum.* **38**, 1545 (1967).

⁵J. Buttet, *Solid State Commun.* **9**, 1129 (1971).

⁶George Mozurkewich, H. I. Ringermacher, and D. I. Bolef, to be published.

⁷R. E. Norberg, *Phys. Rev.* **86**, 745 (1952).

⁸D. E. Schreiber, in *Proceedings of the International Conference on Nuclear Magnetic Resonance and Relaxation in Solids, Thirteenth Colloque Ampère*, edited by L. van Ferven (North-Holland, Amsterdam, 1965), p. 190.

⁹S. Kazama and Y. Fukai, *J. Less-Common Metals* **53**, 25 (1977).

¹⁰D. Zamir and R. M. Cotts, *Phys. Rev.* **134**, A666 (1964).

¹¹H. Lüttgemeir, R. R. Arons, and H. G. Bohn, *J. Magn. Res.* **8**, 74 (1972).

¹²J. R. Franz and M. E. Muller, *Rev. Sci. Instrum.* **48**, 531 (1977).

Possible Observation of Local Plasmon Modes Excited by Electrons Tunneling through Junctions

Arnold Adams, J. C. Wyss, and P. K. Hansma

Department of Physics, University of California, Santa Barbara, California 93106

(Received 16 January 1979)

The light emitted by small-particle tunnel junctions is partially polarized. The excess light polarized perpendicular to the junctions is possibly due to the radiative decay of localized surface plasmons that are excited by tunneling electrons. Both the angular distribution and the intensity versus photon energy of this light are in agreement with recent theoretical calculations based on the excitation and radiative decay of surface plasmons in a small metal particle located above a metal film.

Recently Rendell, Scalapino, and Mühlischlegel calculated the role of local plasmon modes in light emission from small-particle tunnel junctions.¹

A peak in light intensity was predicted at a photon energy near 1.85 eV due to radiative decay of local plasmon modes of gold particles on